ONLINE ONLY

Supplemental material

Normal childhood brain growth and a universal sex and anthropomorphic relationship to cerebrospinal fluid

Peterson et al.

https://thejns.org/doi/abs/10.3171/2021.2.PEDS201006

DISCLAIMER The *Journal of Neurosurgery* acknowledges that the following section is published verbatim as submitted by the authors and did not go through either the *Journal's* peer-review or editing process.

Supplemental Material

Supplemental Methods:

Study Cohort Exclusion Criteria

The NIH Pediatric MRI Repository was collected using exclusion criteria based on neurological examination, family history, behavioral/psychiatric history, physical exam, medical history, pregnancy and birth history, and demographic characteristics. In more detail, any family history of inherited neurological disorders, mental retardation unrelated to trauma in a first-degree relative, or Axis I psychiatric disorder in a first-degree relative qualified a subject for exclusion. Any abnormality found on neurological exam led to exclusion. Language disorders (except simple disarticulation disorders), personal history of an Axis I psychiatric disorder (except for nicotine dependency, enuresis, encopresis, oppositional defiant disorder, simple phobia, social phobia, or adjustment disorder) met exclusion criteria. Subjects scoring less than 70 on the WASI IQ test or Woodcock-Johnson III Achievement Battery subtest and subjects scoring greater than 70 on any Childhood Behavior Checklist for the child of interest subscale were excluded. On physical exam, weight or head circumference below the third percentile (based on the National Health Center for Statistics 2000 data charts) qualified for exclusion. Positive pregnancy test, metal implants that could lead to artifacts on MRI, significant hearing or visual impairment, closed head injury leading to 30 minutes of loss of consciousness or imaging abnormalities, and systemic malignancy necessitating chemotherapy or CNS radiotherapy all necessitated exclusion[1].

Subjects were also excluded if they had a history of a significant medical or neurological disorder such as sickle cell anemia, systemic rheumatologic disease, cluster or migraine headaches, seizure disorder, CNS infection, diabetes, or muscular dystrophy. For demographics, adopted children (due to inadequate family history) and children of parents with limited English proficiency were excluded. Gestational age at birth less than 37 weeks or greater than 42 weeks, hyperbilirubinemia requiring transfusion or more than 2 days of phototherapy, multiple birth, high forceps or vacuum extraction facilitated delivery, C-section for infant or maternal distress, chest compression or intubation for resuscitation after birth, maternal metabolic conditions, general anesthesia during pregnancy or delivery, and significant obstetric complications were included in exclusion criteria. Intra-uterine exposure to substances such as illicit drugs, more

than 2 alcoholic drinks per week during pregnancy, smoking more than ½ pack per day, and certain medications necessitated exclusion[1].

MRI Technical Details

Dual contrast T2-weighted (Fast/Turbo spin echo-ETL/Turbo factor 8, slice thickness 3 mm, oblique axial acquisition, TR 3300 ms, TEl 83 ms, TE2 165 ms, refocusing pulse 180 degrees, field of view and matrix AP: 256 & LR: 192 mm) scans were acquired for infants and Tl-weighted (3D RF-spoiled gradient recalled echo sequence, slice thickness 1 mm to 1.5 mm, sagittal acquisition, TR 22-25 MS, TE 10-11 ms, excitation pulse 30 degrees, whole head field of view, AP 256 matrix with LR for 1 mm isotropic) scans were acquired for adolescents. Each scan in the database was then corrected for intensity non-uniformities using the N3-algorithm in tandem with scanner-specific models of B_0 inhomogeneity from each site[2].

Smoothing Spline analysis of variance (SSANOVA)

Smoothing Spline analysis of variance (SSANOVA) is a semi-parametric method that models data generated from a smooth function $f(x)$ by assuming that f is a function in a Reproducible Kernel Hilbert Space (RKHS) of the form $\mathcal{H} = \mathcal{H}_0 + \mathcal{H}_1$ [3]. The set of functions $(\phi_v(x))_{v=1}^m$, which spans the finite dimensional subspace $\mathcal{H}_0$ and $\mathcal{H}_1$, is a RKHS induced by a given kernel function k. Therefore, f has a semi-parametric form given by

$$f(x) = \sum_{j=1}^{m} d_j \, \phi_j(x) + g(x)$$

for coefficients d_j, where functions ϕ_j have a parametric form and $g \in \mathcal{H}_1$ which is defined by:

$$g(x) = \sum_{\alpha} g_\alpha \, (x_\alpha) + \sum_{\alpha<\beta} g_{\alpha\beta} \, (x_\alpha, x_\beta) + \cdots$$

where g_α and $g_{\alpha\beta}$ satisfy the standard ANOVA side conditions.

The SS-ANOVA estimate of f given data $(x_i, y_i), i = 1, \ldots, n,$ is given by the solution of a penalized problem,

$$\min_{f \in H} (y_t - f(x))^2 + \lambda J(f(x)) \qquad (1)$$

where the first term discourages the lack of fit of f and the second term penalizes the complexity of f with smoothing parameter λ controlling the trade-off between the two.

Following the representor theorem of Kimeldorf et al (1970)[4] and the assumption of Gaussian data, the minimizer of the problem in equation (1) has a finite representation of the form:

$$f(x) = \sum_{v=1}^{m} d_v \, \phi_v(x) + \sum_{j=1}^{n} c_j \, k(x_j, x)$$

for coefficients c_i and d_v.

Letting Y be the matrix of observations of size $N \times 1$, where N includes all observations, including repeated measurements for different subjects; S is a $N \times m$ matrix where m represents the number of unpenalized terms in the model; and Q is a $N \times N$ matrix which accounts for all penalized terms in the model; estimation reduces to:

$$\min_{d,c} (Y - Sd - Qc)^T (Y - Sd - Qc) + n\lambda c^T Q c.$$

Here S is the matrix described above with the iv^{th} entry being $\phi_v(x_i)$ and Q is the penalized matrix with the ij^{th} entry being $k(x_i, x_j)$[5]. We use Generalized Approximate Cross-Validation (GACV), an approximation to the leave-one-out estimate of the comparative Kullback-Leibler distance between the empirical data $\hat{f}$ and the unknown true f to select regularization parameter λ and θ. This is dependent on the data available.

We were interested in visualizing and statistically analyzing the longitudinal differences between hemispheres, and therefore incorporated hemisphere as a main factor rather than a nested factor. Furthermore, some subjects only had one data point collected, while others had two or three. This imbalance and the low levels of repetition lead to matrix rank-deficiency in modeling hemisphere as a nested variable, rendering the nested approach mathematically inappropriate for this dataset.

Generalized Additive Models for Location, Scale, and Shape (GAMLSS)

The smooth growth curves used to fit the volumes and other growth metrics included in this study were developed using the Generalized Additive Models for Location, Scale, and Shape software implemented in R[6]. The Box-Cox power exponential (BCPE) distribution, which was chosen by the World Health Organization (WHO) for their standard growth curves, was used to model the volumes in this study[7]. This distribution models the median for a nonparametric assessment, and appropriately accounts for kurtosis and skewness within the data. The growth

curves were fitted using the default RS algorithm and were smoothed using fractional polynomials of the third order[6].

Segmentation

The neonates and infants were assessed using the Developing Human Connectome Project (dHCP) pipeline, which required T2 images and was run through a virtual Docker container to access a Linux computer system[8]. The dHCP pipeline relies on the Brain Extraction Tool (BET) algorithm for skull-stripping, followed by the N4 algorithm for intensity inhomogeneity correction and the Draw-EM algorithm for segmentation [9-11]. The Draw-EM (Developing brain Region Annotation With Expectation-Maximization) algorithm consists of an adaptive Expectation-Maximization scheme relying on a spatial prior term and intensity model. The spatial prior term is established using labeled atlases that are registered to the image, whereas the intensity model is established using a Gaussian Mixture Model. A partial volume correction is applied to the CSF and white matter due to the similar intensity profile, particularly along the CSF and cortical grey matter boundaries[8]. Furthermore, label fusion and EM model averaging are applied to discern between structures that share boundaries characterized by similar intensity profiles[8]. The labeled atlases were obtained through manual editing and later updated by Markopoulos et al[11, 12].

The older subjects were assessed using the Computational Anatomy Toolbox 12 (CAT12) within the Statistical Parametric Mapping (SPM) platform using Matlab 2019b, which relies on T1 images[13]. The CAT12 algorithm relies on voxel-based morphometry for segmentation and label-based morphometry for region-of-interest (ROI) classification. Each scan was preprocessed using a modified ICBM Tissue Probabilistic Atlas tissue probability map along with an ICBM space template affine registration. Skull-stripping was accomplished using adaptive probability region-growing (APRG) algorithm followed by surface-based optimization. The MNI152 Dartel Template was used for Dartel registration, and finally the Hammers atlas was used for ROI analysis[14]. Each of the resulting scan sets was manually curated to ensure that appropriate skull-stripping and segmentation was accomplished. Upon establishing the volumes determined by each segmentation procedure, the accompanying atlases were used to compile volumes for the desired regions from smaller sections of the brain[11, 12, 14].

Upon establishing the volumes determined by each segmentation procedure, the accompanying atlases were used to compile volumes for the desired regions from smaller sections of the brain[11, 12, 14].

Supplemental Figures:

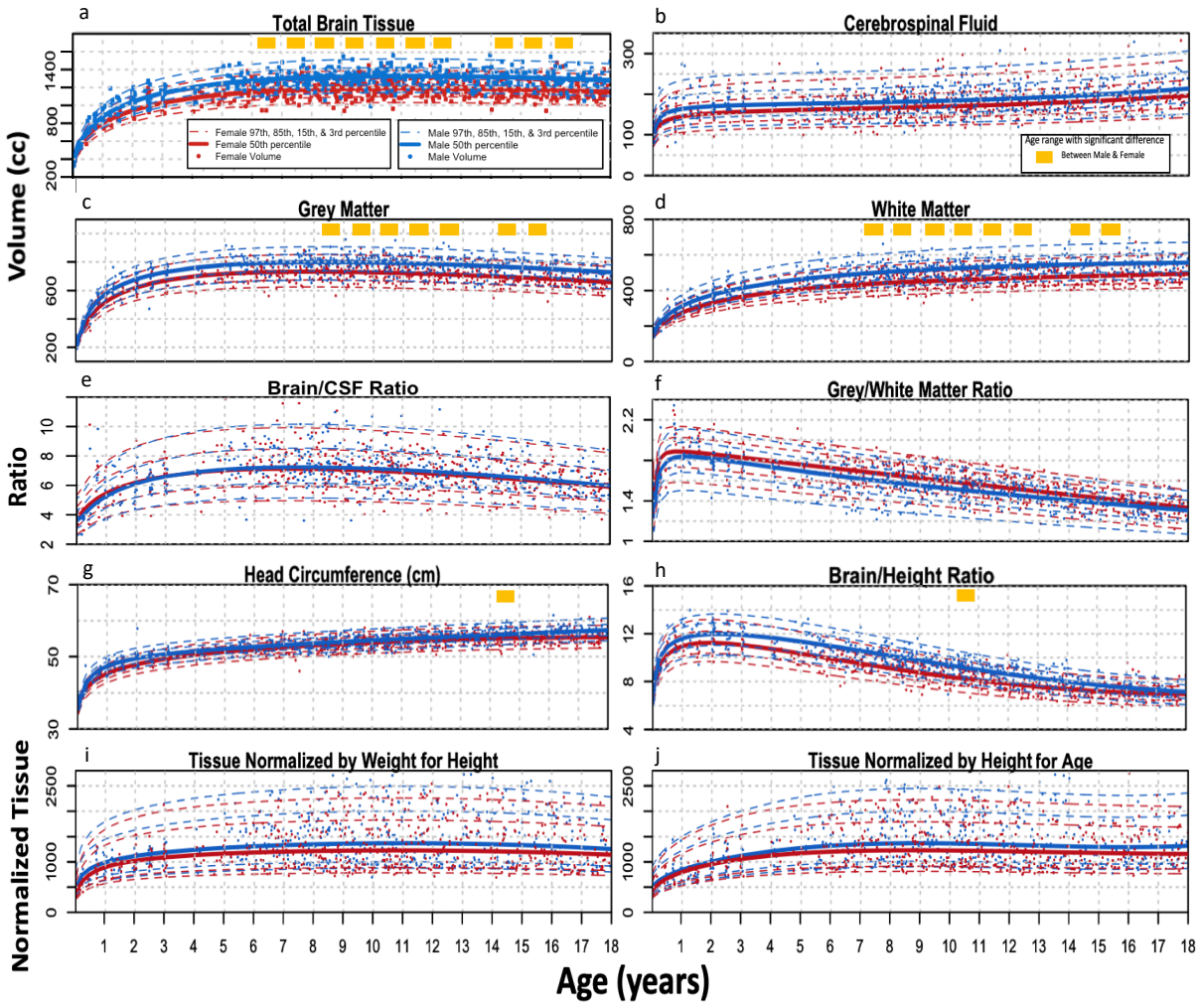

Supplemental Figure 1. Brain Component Standard Growth Curves. Growth curves from birth to 18-years-old developed with Generalized Additive Models for Location, Shape, and Scale are shown for males in blue and females in red, with the solid median accompanied by dotted one and two standard deviations above and below. Each growth curve was modeled using a Box-Cox power exponential distribution and smoothed using fractional polynomials. The yellow boxes represent Bonferroni corrected significant differences ($p<0.00006$) between males and females for each year, obtained using the Mann-Whitney test. This univariate testing was applied to obtain conservative estimates of the differences in the data for each year of life. The standard curves plotted include **a)** total brain volume (cc), **b)** CSF, **c)** grey matter, **d)**white matter, **e)** the ratio of total brain volume to CSF, **f)** the ratio of grey to white matter, **g)** head circumference (cm), **h)** height normalized brain volume, **i)** weight for height normalized brain volume, and **j)** height for age normalized brain volume.

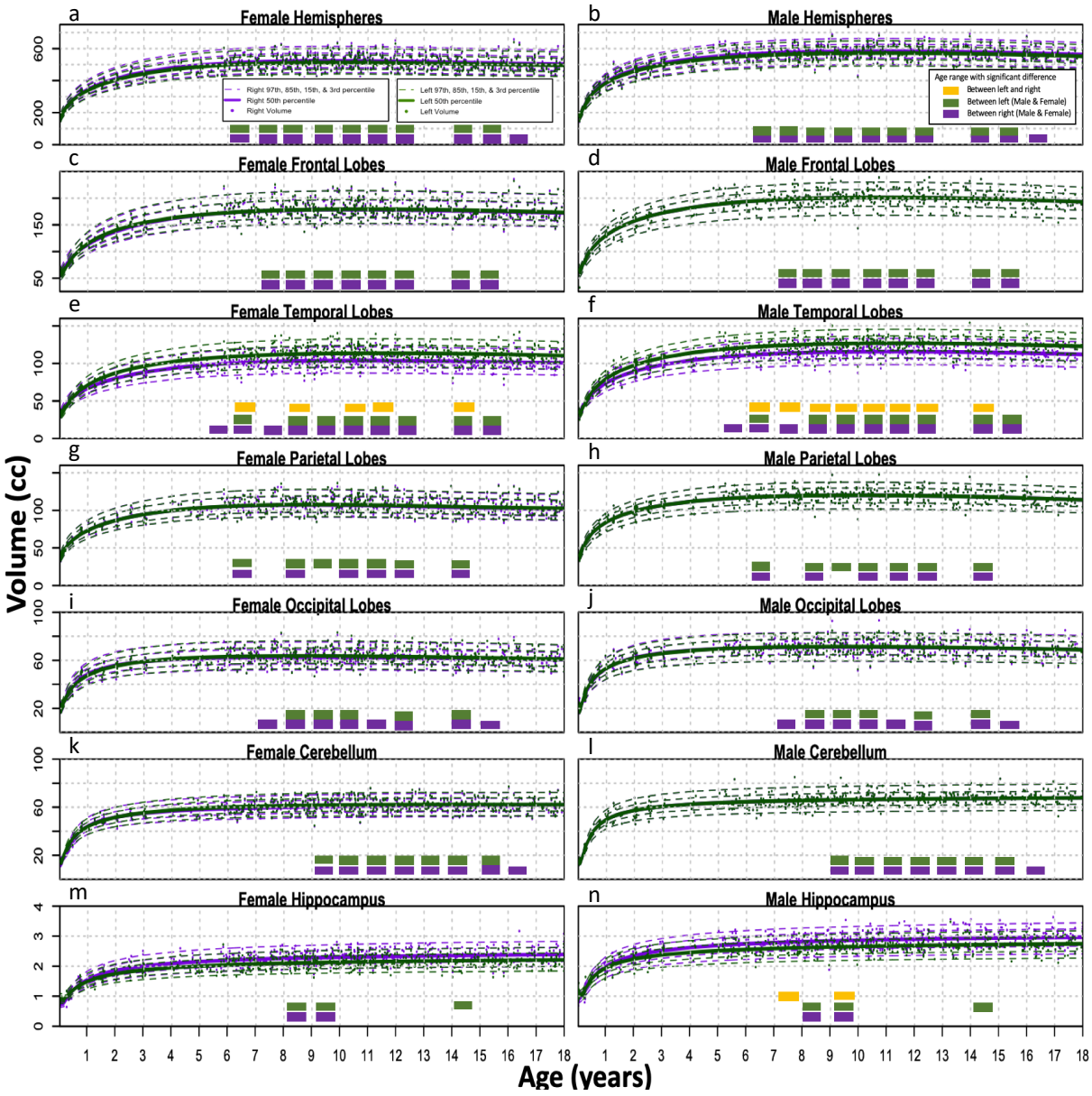

Supplemental Figure 2. Brain Region Standard Growth Curves. Female regional growth curves from birth to 18-years-old are shown in the left column, and the corresponding male regional curves are shown in the right column, all developed using Generalized Additive Models for Location, Shape, and Scale. Each growth curve was modeled using a Box-Cox power exponential distribution and smoothed using fractional polynomials. Left regions are shown in green, and right regions are shown in purple, with the solid median accompanied by dotted one and two standard deviations above and below. The yellow boxes represent Bonferroni corrected significant differences ($p<0.00006$) between left and right components in that year, obtained using the Mann-Whitney test. The green boxes represent significant differences between the left region for males and females in that year, while the purple boxes represent significant differences between the right region for males and females in that year. The standard curves plotted include **(a,b)** hemispheres (cc), **(c,d)** frontal lobes (cc), **(e,f)** temporal lobes (cc), **(g,h)** parietal lobes (cc),**(i,j)** occipital lobes (cc), **(k,l)** cerebella (cc), and **(m,n)** hippocampi (cc).

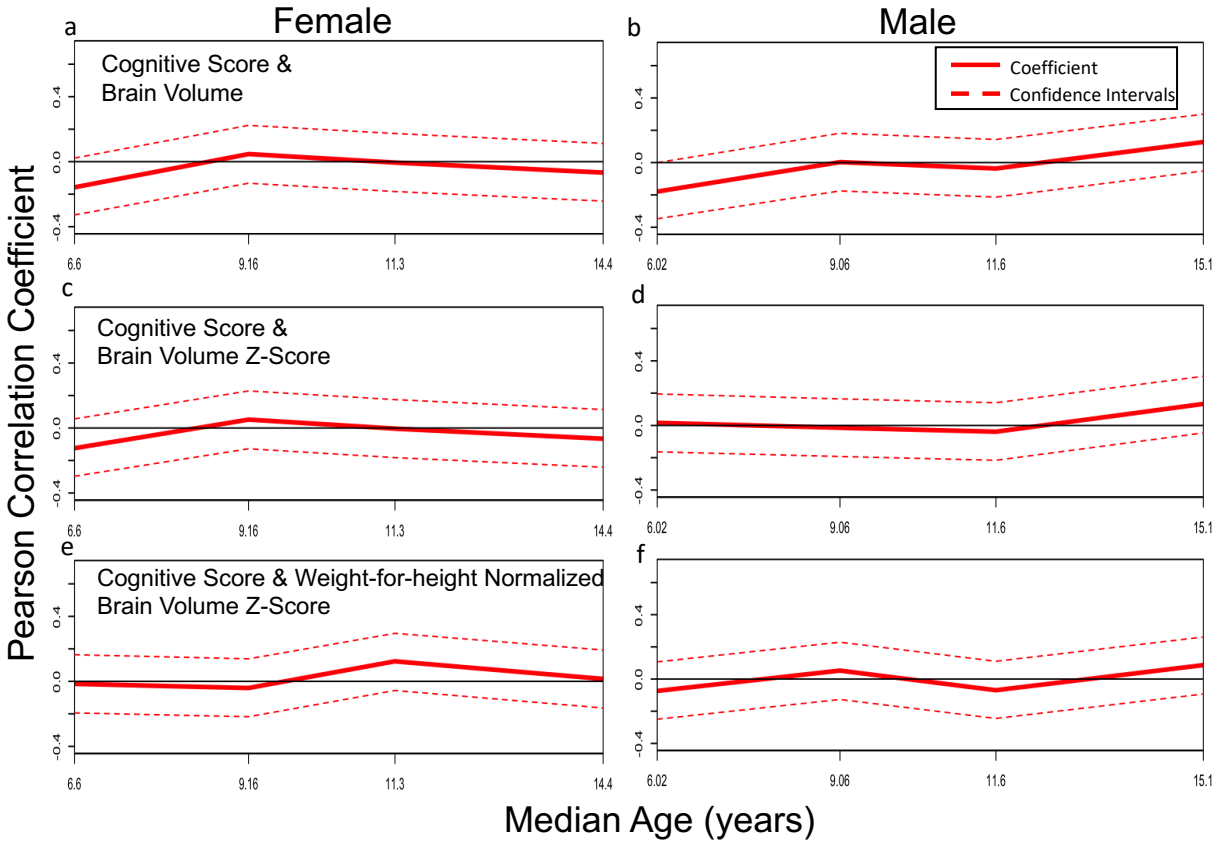

Supplemental Figure 3. Cognitive Score Correlations by Sex. Age-dependent correlations were calculated with a subpopulation window-size of 120 and step-size of 20 subjects to show the Pearson Correlation and confidence intervals between cognitive score and **(a,b)** raw brain volume, **(c,d)** brain volume z-score, and **(e,f)** weight-for-height normalized brain volume z-score at different ages for both females and males.

Supplemental References:

1. Evans AC. The NIH MRI study of normal brain development. *NeuroImage*. 2006/03/01/ 2006;30(1):184-202. doi:https://doi.org/10.1016/j.neuroimage.2005.09.068
2. Sled JG, Zijdenbos AP, Evans AC. A nonparametric method for automatic correction of intensity nonuniformity in MRI data. *IEEE Trans Med Imaging*. Feb 1998;17(1):87-97. doi:10.1109/42.668698
3. Craven P, Wahba G. Smoothing noisy data with spline functions. *Numer Math*. 1978/12/01 1978;31(4):377-403. doi:10.1007/BF01404567
4. Kimeldorf GS, Wahba G. A Correspondence Between Bayesian Estimation on Stochastic Processes and Smoothing by Splines. *Ann Math Stat*. 1970/04 1970;41(2):495-502. doi:10.1214/aoms/1177697089
5. Golub GH, Heath M, Wahba G. Generalized Cross-Validation as a Method for Choosing a Good Ridge Parameter. *Technometrics*. 1979;21(2):215-223. doi:10.2307/1268518
6. Rigby RA, Stasinopoulos DM, Lane PW. Generalized additive models for location, scale and shape. *J R Stat Soc Ser C Appl Stat*. 2005;54(3):507-554. doi:10.1111/j.1467-9876.2005.00510.x
7. Rigby RA, Stasinopoulos DM. Smooth centile curves for skew and kurtotic data modelled using the Box-Cox power exponential distribution. *Stat Med*. Oct 15 2004;23(19):3053-76. doi:10.1002/sim.1861
8. Makropoulos A, Robinson EC, Schuh A, et al. The developing human connectome project: A minimal processing pipeline for neonatal cortical surface reconstruction. *Neuroimage*. Jun 2018;173:88-112. doi:10.1016/j.neuroimage.2018.01.054
9. Smith SM. Fast robust automated brain extraction. *Hum Brain Mapp*. Nov 2002;17(3):143-55. doi:10.1002/hbm.10062
10. Tustison NJ, Avants BB, Cook PA, et al. N4ITK: improved N3 bias correction. *IEEE Trans Med Imaging*. Jun 2010;29(6):1310-20. doi:10.1109/TMI.2010.2046908
11. Makropoulos A, Gousias IS, Ledig C, et al. Automatic whole brain MRI segmentation of the developing neonatal brain. *IEEE Trans Med Imaging*. Sep 2014;33(9):1818-31. doi:10.1109/TMI.2014.2322280
12. Gousias IS, Edwards AD, Rutherford MA, et al. Magnetic resonance imaging of the newborn brain: Manual segmentation of labelled atlases in term-born and preterm infants. *NeuroImage*. 2012/09/01/ 2012;62(3):1499-1509. doi:https://doi.org/10.1016/j.neuroimage.2012.05.083
13. Gaser C, Dahnke R. CAT-a computational anatomy toolbox for the analysis of structural MRI data. 2016;2016:336-348.
14. Hammers A, Allom R, Koepp MJ, et al. Three-dimensional maximum probability atlas of the human brain, with particular reference to the temporal lobe. *Hum Brain Mapp*. 2003;19(4):224-247. doi:10.1002/hbm.10123

Supplemental Growth Chart

Normal brain growth and CSF accumulation curves, and brain/CSF ratio, from birth to age 18 for males and females. A high resolution reproduction of Figure 6 from the main paper.

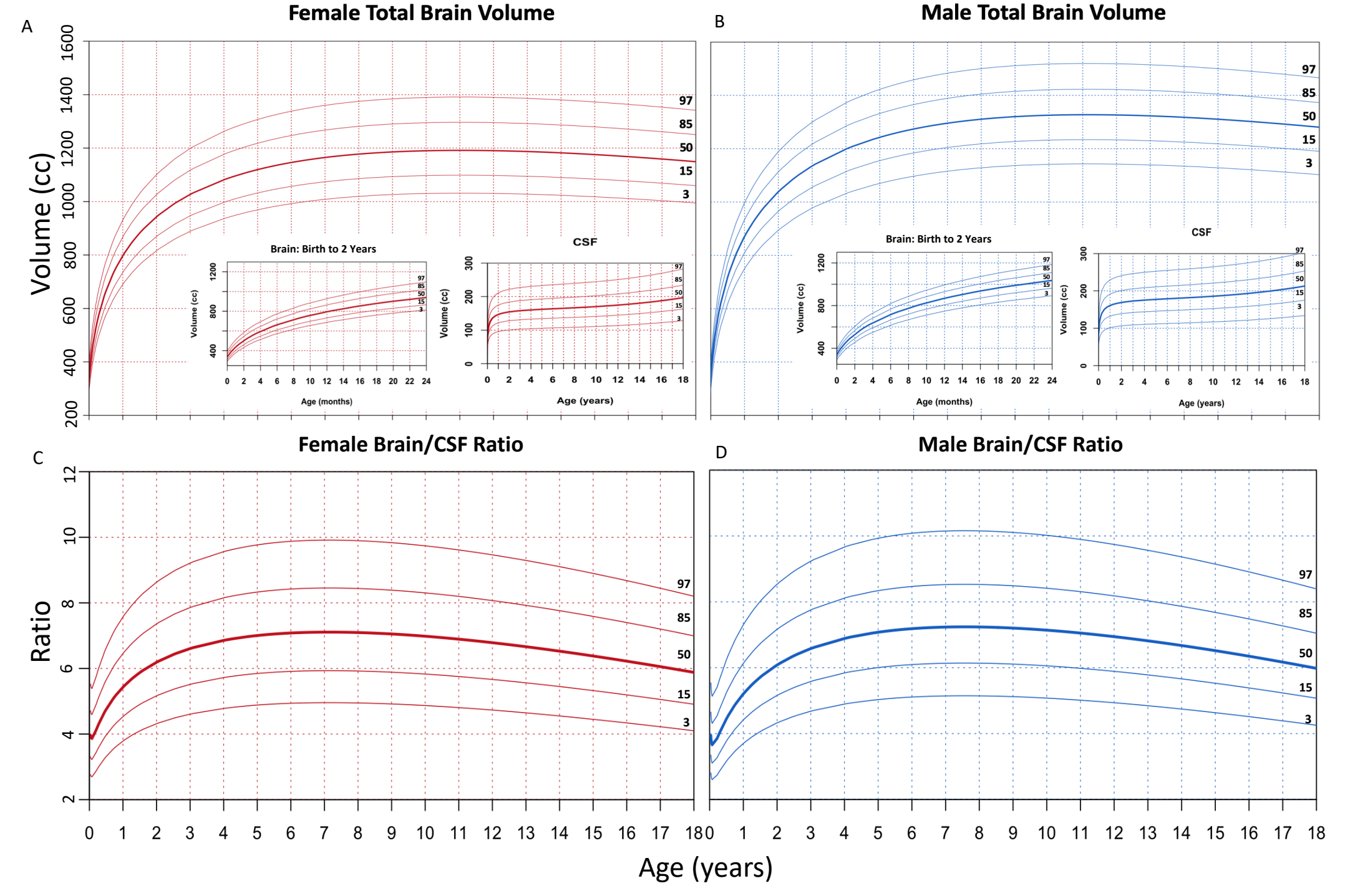
A
Female Total Brain Volume
Volume (cc)
200
400
600
800
1000
1200
1400
1600
97
85
50
15
3
Brain: Birth to 2 Years
Volume (cc)
400
800
1200
0 2 4 6 8 10 12 14 16 18 20 22 24
Age (months)
CSF
Volume (cc)
0
100
200
300
0 2 4 6 8 10 12 14 16 18
Age (years)
B
Male Total Brain Volume
97
85
50
15
3
Brain: Birth to 2 Years
Volume (cc)
400
800
1200
0 2 4 6 8 10 12 14 16 18 20 22 24
Age (months)
CSF
Volume (cc)
0
100
200
300
0 2 4 6 8 10 12 14 16 18
Age (years)
C
Female Brain/CSF Ratio
Ratio
2
4
6
8
10
12
97
85
50
15
3
D
Male Brain/CSF Ratio
97
85
50
15
3
0 1 2 3 4 5 6 7 8 9 10 11 12 13 14 15 16 17 18
0 1 2 3 4 5 6 7 8 9 10 11 12 13 14 15 16 17 18
Age (years)